MOL PHARM

MOLECULAR PHARMACOLOGY

Structural Basis for Competition between Drug Binding and Kvβ1.3 Accessory Subunit-Induced N-Type Inactivation of Kv1.5 Channels

Niels Decher, Pradeep Kumar, Teresa Gonzalez, Vijay Renigunta, and Michael C. Sanguinetti

From the Nora Eccles Harrison Cardiovascular Research and Training Institute and Department of Physiology, University of Utah, Salt Lake City, Utah (N.D., P.K., T.G., M.C.S.); and Institut für Normale und Pathologische Physiologie, Universität Marburg, Marburg, Germany (V.R.)

ABSTRACT

Kvβ subunits are accessory proteins that modify gating of Kv1 channels. Kvβ1.3 subunits bind to the N termini of Kv1.5 α-subunits and induce fast N-type inactivation, slow the rate of deactivation, and alter the voltage dependence and kinetics of channel activation. The N terminus of a Kvβ subunit and quaternary ammonium compounds bind to the inner pore of Kv1 channels; however, it is unknown to what extent the pore binding sites for drugs and Kvβ subunits overlap. Here, we used site-directed Ala mutagenesis to scan residues of the Kv1.5 pore to define the binding site for Kvβ1.3 subunits. Individual mutations of five residues in the S6 domain (Val505, Ile508, Leu510, Val512, and Val516) greatly retarded or prevented Kvβ1.3 induced inactivation, and reduced effects on Kv1.5 deactivation. Mutation of Thr479 and Thr480 enhanced Kvβ1.3-induced N-type inactivation. None of the Ala mutations prevented the Kvβ1.3-induced negative shifts in the voltage dependence of activation or slow C-type inactivation, suggesting that these gating effects are mediated by an interaction other than the one for N-type inactivation. Thr479, Thr480, Val505, Ile508, and Val512, of Kv1.5 channels are also important interaction sites for the anthranilic acid S0100176 (N-benzyl-N-pyridin-3-ylmethyl-2-(toluene-4-sulfonylamino)-benzamide hydrochloride). Leu510 and V516A prevented Kvβ1.3-induced inactivation but did not alter drug block. Block of Kv1.5 by S0100176 was reduced and voltage-dependent in the presence of Kvβ1.3 but not in the presence of an N-truncated form of the Kvβ subunit. Thus, residues in the pore of Kv1.5 required for N-type inactivation overlap with but are not identical to the drug binding site.

Voltage gated K⁺ (Kv) channels have diverse cellular functions, including maintenance of the resting potential, repolarization of action potentials, indirect modulation of neurohormone release, volume regulation, and K⁺ transport. Kv channels are formed by coassembly of four pore-forming α-subunits. The diversity of Kv channel structure and function is enhanced by heteromultimerization of different α-subunits (Coetzee et al., 1999) or by coassembly with small accessory Kvβ subunits (Rhodes et al., 1997). Kvβ subunits can bind to Kv α-subunits to form $\alpha_4\beta_4$ complexes that modify the biophysical properties and/or expression levels of the heteromultimeric channel. For ex-

ample, Kv1.5 α-subunits form delayed rectifier K⁺ channels that activate in response to membrane depolarization and slowly inactivate by a "C-type" mechanism involving the pore helix and S6 domains. Kvβ subunits bind to the N terminus of Kv1 subunits and induce a comparatively rapid "N-type" inactivation (Hoshi et al., 1990; Zagotta et al., 1990; Sewing et al., 1996). In addition, Kvβ1.2 (De Biasi et al., 1997) and Kvβ1.3 (Uebele et al., 1998) subunits slow the rate of Kv1.5 channel deactivation and cause a negative shift in the voltage dependence of activation and inactivation gating. Kvβ2 subunits bind to the C termini of Kv2.2 or Kv4.3 channels to increase their cell surface expression without obvious effects on gating properties (Fink et al., 1996; Yang et al., 2001). Kvβ3.1 subunits confer inactivation to Kv1.5 channels that is much faster and more complete than other Kvβ subunits (Leicher et al., 1998). Knockout of Kvβ1.1 in the mouse

ABBREVIATIONS: S0100176, N-benzyl-N-pyridin-3-ylmethyl-2-(toluene-4-sulfonylamino)-benzamide hydrochloride; WT, wild-type; ΔN1–10, deletion of 10 N-terminal amino acids; TBA, tetrabutylammonium.

reduced inactivation of A-type current, reduced the slow after-hyperpolarization and caused frequency-dependent spike broadening in hippocampal CA1 pyramidal neurons and impaired memory (Giese et al., 1998). Thus, accessory Kvβ subunits can fine-tune the membrane stabilizing function of a variety of Kv channels by modifying their biophysical properties or trafficking to the cell surface.

N-type inactivation occurs by a "ball-and-chain"-type mechanism (Armstrong, 1981), where the ball is formed by the N terminus of a Kv channel α-subunit (Hoshi et al., 1990). Some channels exhibit fast inactivation only when a Kvβ subunit is tethered to a specific region of the N terminus of the pore-forming α-subunit. In these channels (e.g., Kv1.5), the N terminus of the Kvβ subunit acts as the ball structure. Based on NMR structures, it was proposed that the ball peptide of Kv α-subunits forms a compact hairpin structure that binds to the inner vestibule to physically occlude the pore similar to a shallow plug (Antz et al., 1997; Antz and Fakler, 1998). Chimeric Kv$\beta2$/Kv$\beta1.1$ subunits can coassemble with N terminus-deleted Kv1.4 α-subunits to induce rapid N-type inactivation. In this case, it was proposed that the N terminus of the Kvβ subunit enters the channel pore as an extended peptide similar to a deep plug (Zhou et al., 2001). It is unclear whether this mechanism applies to other Kvβ and Kv α-subunits. For example, the structure of Kv$\beta1.3$ differs markedly from Kv$\beta1.1$ and is less lipophilic than most inactivation ball peptides in that it contains one charged and one polar amino acid within the first six residues.

Kv1 channels are molecular targets for investigational therapeutic agents. Kv1.5 channel blockers have been proposed for treatment of atrial arrhythmias (Snyders and Yeola, 1995; Peukert et al., 2003) and Kv1.3 blockers are under investigation as immunosuppressants (Hanner et al., 2001; Vennekamp et al., 2004). In addition to altering Kv1 channel gating and expression, coassembly with Kvβ subunits can modulate their pharmacology. For example, Kv$\beta1.3$ subunits reduce the block of Kv1.5 by bupivacaine and quinidine (Gonzalez et al., 2002); however, it remains unclear whether drugs compete with Kvβ subunits for a common binding site on the Kv1.5 channel (Uebele et al., 1998).

We previously used an Ala-scanning mutagenesis approach to define residues in the pore of Kv1.5 that interact with S0100176, an open channel blocker (Decher et al., 2004). Mutation of Thr479 and Thr480 located at the base of the pore helix and Val505, Ile508, and Val512, located in the S6 domain in positions that face the inner pore, had the greatest effect on reducing the potency of drug-induced block of Kv1.5 channels. In this study, we use Ala-scanning mutagenesis and voltage clamp analysis of mutant Kv1.5 channels expressed in *Xenopus laevis* oocytes to identify pore residues that interact with Kv$\beta1.3$. Several mutations abolished Kv$\beta1.3$-induced N-type inactivation and slow deactivation. Two mutations enhanced the effects of Kv$\beta1.3$. Most of the Kv1.5 mutations that affected the functional interactions with Kv$\beta1.3$ also reduced block by S0100176. Our findings provide a refined structural basis for the mechanisms of Kv$\beta1$-induced N-type inactivation of

Kv1.5 channels and competition between drug-binding and N-type inactivation.

Materials and Methods

Molecular Biology. Site-directed mutation of Kv1.5 subcloned into the pSGEM oocyte expression vector was described previously (Sarkar and Sommer, 1990). The latest database entry for the sequence of Kv1.5 (GenBank accession number NM_002234) contains two additional residues in the N terminus compared with the original sequence (GenBank M60451). Thus, the amino acid numbering used here and in our previous work (Decher et al., 2004) is +2 greater compared with the numbering in most of the existing Kv1.5 literature. Restriction mapping and DNA sequencing of the PCR-amplified segment were used to confirm the presence of the desired mutation and the lack of extra mutations in Kv1.5. cRNA for injection into oocytes was prepared with T7 Capscribe (Roche, Indianapolis, IN) after linearization with NheI. The Kv$\beta1.3$ construct in a modified pSP64T vector and the creation of amino-terminal deletion mutants was described previously (England et al., 1995; Uebele et al., 1998). cRNA was made with SP6 Capscribe (Roche) after linearization with EcoRI. Estimates of cRNA quality and quantity were determined by gel electrophoresis and UV spectroscopy.

Isolation, Injection, and Voltage Clamp of Oocytes. Stage IV and V *Xenopus laevis* oocytes were isolated and injected with cRNA encoding wild-type (WT) or mutant Kv1.5 channels. Oocytes were injected with 5.0 to 12.5 ng of Kvβ and/or 2.5 to 12.5 ng of Kv1.5 cRNA, then cultured in Barth's solution supplemented with 50 μg/ml gentamicin and 1 mM pyruvate at 18°C for 1 to 3 days before use in voltage clamp experiments. Barth's solution contained 88 mM NaCl, 1 mM KCl, 0.4 mM CaCl$_2$, 0.33 mM Ca(NO$_3$)$_2$, 1 mM MgSO$_4$, 2.4 mM NaHCO$_3$, and 10 mM HEPES, pH 7.4. For voltage-clamp experiments, oocytes were bathed in a modified ND96 solution containing 96 mM NaCl, 4 mM KCl, 1 mM MgC1$_2$, 1 mM CaC1$_2$, and 5 mM HEPES, pH 7.6. Currents were recorded at room temperature (23−25°C) with standard two-microelectrode voltage-clamp techniques (Stuhmer, 1992). The holding potential was −80 mV and the interpulse interval for all voltage clamp protocols was 10 s or slower to allow channels to fully recover from inactivation between pulses. To obtain current-voltage relationships and activation curves, 200 ms voltage steps were applied in 10 mV increments to potentials that varied from −60 to +70 mV, followed by repolarization to −40 mV to record tail currents.

Data analysis. pCLAMP 8 (Axon Instruments), and Origin 7 (Microcal Software) software were used for data acquisition and analysis on a Dell Optiplex GX150 PC. The voltage dependence of Kv1.5 channel activation (with or without coexpression with Kv$\beta1.3$) was determined from tail current analyses at −40 mV. The plot of current amplitude versus test potential was fit to a Boltzmann equation to obtain the half-point ($V_{1/2}$) and slope factor (k) for the relationship: $I_n = 1/(1 + \exp[(V_{1/2} - V_t)/k])$.

The voltage dependence of Kv1.5 inactivation was determined by using a two-pulse protocol. A prepulse of 1 s was applied to potentials ranging from −90 to +70 mV and was immediately followed by a 200-ms test pulse to +70 mV. For T480A Kv1.5 channels, pulses were applied up to +130 mV. The relative amplitude of peak current during the test pulse was plotted as a function of the prepulse voltage and the relationship fit to a Boltzmann function to obtain the $V_{1/2}$ for inactivation. Other voltage pulse protocols are described under *Results* and in the figure legends. Data are expressed as mean ± S.E.M. (n = number of oocytes).

Drugs. S0100176 was synthesized by the medicinal chemistry-department of Aventis Pharma Deutschland GmbH (Bad Soden, Germany). The drug was prepared as a 50 mM stock solution in dimethyl sulfoxide and stored at room temperature.

Results

Mutations of Specific Residues in Kv1.5 Alter the Functional Response to Kvβ1.3. When expressed alone in oocytes, Kv1.5 subunits coassemble to form channels that conduct a rapid outward K$^+$ current that is activated by depolarization of the oocyte to potentials greater than -20 mV. Currents were characterized by voltage clamping the membrane for 200 ms to potentials ranging from -60 to $+70$ mV from a holding potential of -80 mV (Fig. 1A). WT Kv1.5 current exhibited no detectable inactivation in response to such short pulses; however, 5-s pulses to $+70$ mV revealed a slow C-type inactivation that was well described by a biexponential function with time constants of 5.48 ± 0.73 s and 586 ± 54 ms ($n = 7$, data not shown). Coexpression of Kv1.5 with Kvβ1.3 subunits induced an

additional, rapid N-type inactivation with an average fast time constant (τ_{fast}) of 4.7 ± 0.2 ms and a slow time constant (τ_{slow}) of 173.2 ± 9.8 ms ($n = 14$). In addition, Kvβ1.3 induced a slowing of Kv1.5 deactivation, observed as a slowly decaying tail current when the membrane was returned to a potential of -40 mV (Fig. 1A).

We used a site-directed mutagenesis approach to identify residues in the S6 domain and pore helix that might interact with Kvβ1.3 subunits. Twenty-two amino acids in the S6 domain and two amino acids located at the base of the pore helix (Thr479, Thr480) were individually mutated to Ala. Native Ala residues were mutated to Val. Four mutations (G504A, A509V, P511A, and I515A) rendered the channel nonfunctional, preventing further evaluation. The other 20 mutant channels expressed robust currents
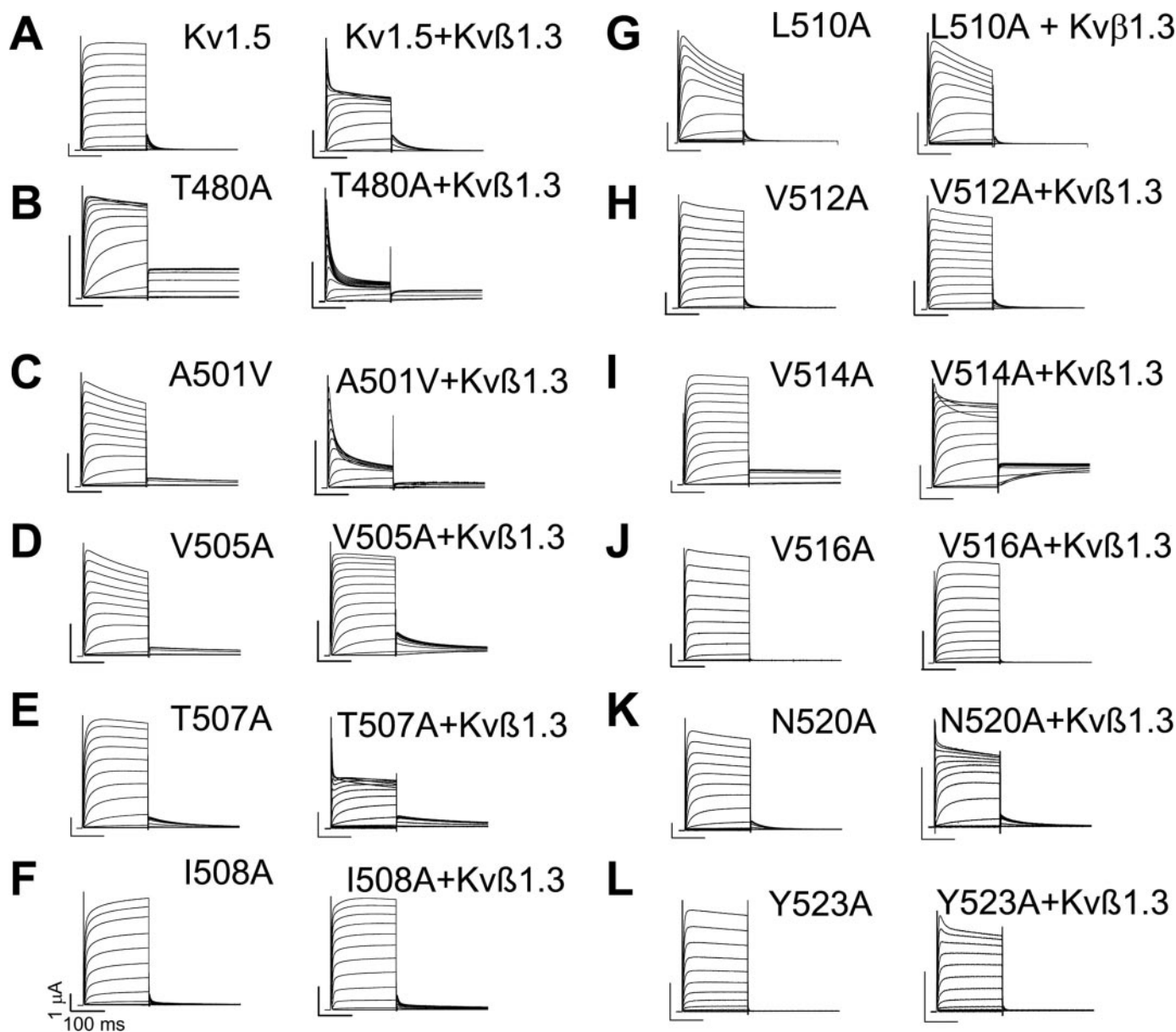

Fig. 1. Effects of Kvβ1.3 on wild-type and mutant Kv1.5 channels expressed in *X. laevis* oocytes. A to L, current traces recorded during 200-ms pulses to potentials ranging from -60 to $+70$ mV from a holding potential of -80 mV. Tail currents were recorded upon return of the membrane potential to -40 mV. Left, currents recorded from oocytes expressing Kv1.5 subunits alone. Right, currents recorded from oocytes expressing Kv1.5 subunits and Kvβ1.3 subunits. Point mutations in Kv1.5 subunits are indicated above current tracings.

in oocytes. Examples of currents conducted by mutant Kv1.5 channels expressed with or without Kvβ1.3 subunits are illustrated in Fig. 1, B to L. Some mutations, for example T480A, A501V, and V505A enhanced the rate of C-type inactivation and slowed the rate of deactivation of Kv1.5 even in the absence of Kvβ1.3 subunits (Fig. 1, B–D).

V514A (Fig. 1I) slowed deactivation without a change in inactivation. Other mutations (e.g., I508A, V512A, V516A, N520A, and Y523A; Fig. 1, F, H, and J–L) induced only minor changes in gating compared with WT Kv1.5. Coexpression of mutant Kv1.5 channels with Kvβ1.3 subunits had a widely variable effect on inactivation properties. For
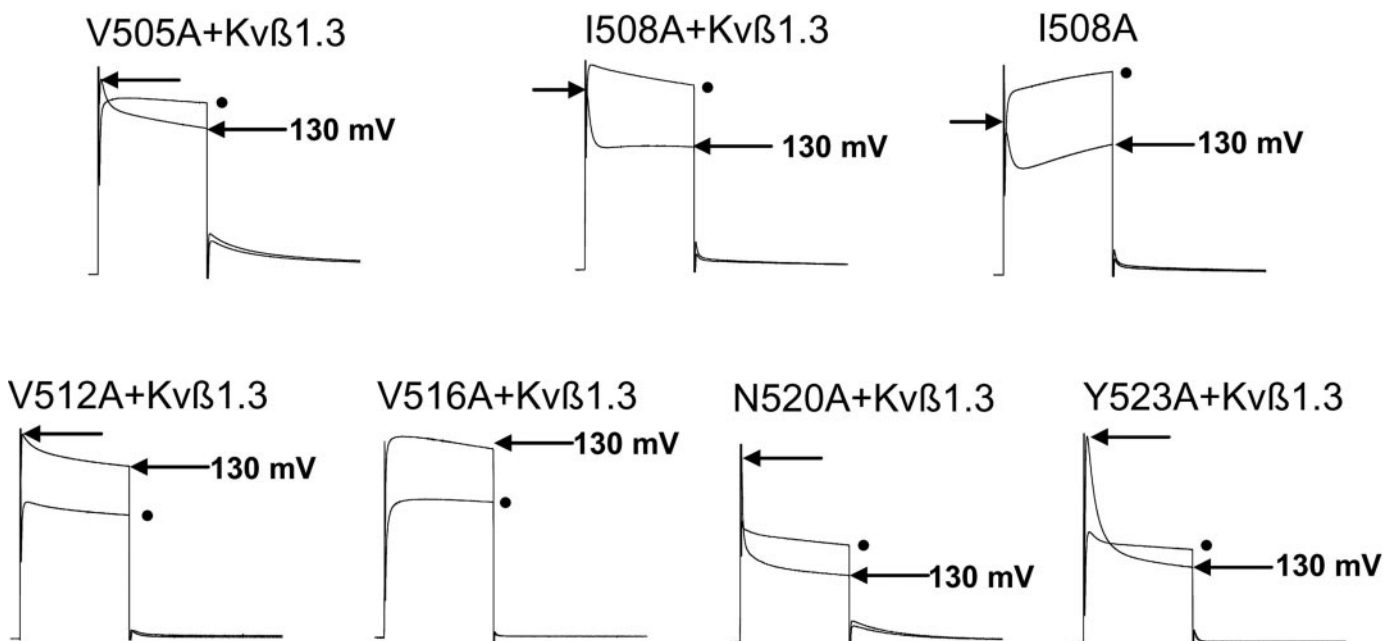
Fig. 2. Inactivation for some mutant Kv1.5 mutant channels coexpressed with Kvβ1.3 occurs only at very depolarized potentials. Currents were recorded during 200-ms pulses to test potentials of +70 mV (●) and +130 mV (indicated by arrows). Note that Kvβ1.3 did not induce additional inactivation of I508A Kv1.5 channels. Point mutations in Kv1.5 subunits are indicated above current tracings.
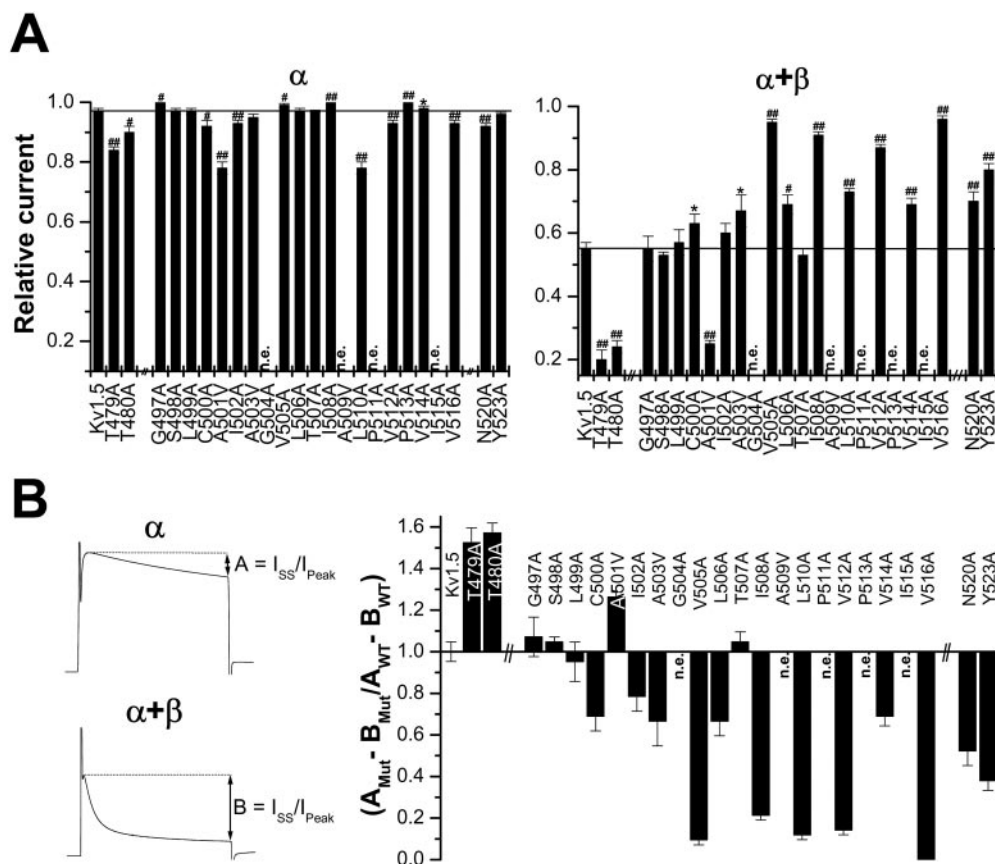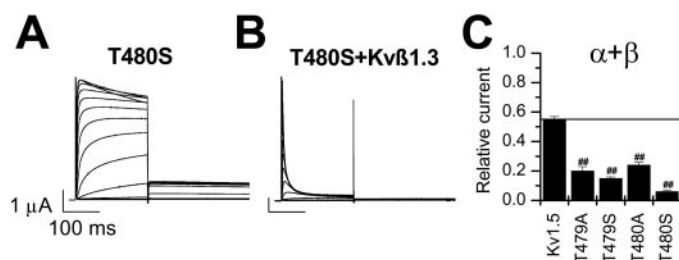

Fig. 3. Inactivation of mutant Kv1.5 channels expressed alone or coexpressed with Kvβ1.3 subunits. A, current measured at the end of 200-ms pulses to +70 mV was normalized relative to the peak initial current to obtain relative current for WT and mutant Kv1.5 channels expressed in oocytes alone (left) or when coexpressed with Kvβ1.3 subunits (right). P513A Kv1.5/Kvβ1.3 channels did not express at levels sufficient to permit measurement. *, $P < 0.05$; #, $P < 0.01$; ##, $P < 0.001$ compared with WT Kv1.5 (left) or WT Kv1.5+Kvβ1.3 (right). B, additional (N-type) inactivation-mediated reduction of Kv1.5 channel current caused by coexpression with Kvβ1.3, expressed as a ratio of relative currents calculated as indicated in inset shown at left. I_{SS}, current at end of 200 ms pulse to +70 mV; I_{Peak}, peak initial current; n.e., no expression (A509V channels expressed very small currents and were not analyzed).

example, inactivation of T480A Kv1.5 was greatly enhanced by Kvβ1.3 (Fig. 1B), but Kvβ-subunits did not induce rapid inactivation of V505A, I508A, L510A, V512A, or V516A mutant channels when examined with test potentials as positive as +70 mV (Fig. 1). Each of these S6 residues, except Leu510 (a residue conserved in other Kv channels), is predicted to face the central cavity of the channel based on homology with the bacterial KcsA channel (Doyle et al., 1998). Mutation of the Asn520 and, in particular, Tyr523 residues, predicted to face the central pore but located at a more distal location in the S6 segment, also reduced the ability of Kvβ1.3 to induce inactivation (Fig. 1, K and L). Val505, Asn520, and Tyr523 mutant channels coexpressed with Kvβ1.3 exhibited significant inactivation when pulsed to +130 mV. However, even at this very depolarized potential, V512A and V516A channels resisted N-type inactivation, and I508A exhibited no additional Kvβ1.3-induced inactivation (Fig. 2). In summary, Kvβ1.3-induced N-type inactivation results from interaction with only a few Kv1.5 residues located at the base of the pore helix and in the S6 domain. With one exception (Leu510), these key residues face toward the central cavity of the channel.

The extent of inactivation of Kv1.5 channels when expressed with or without Kvβ1.3 subunits is summarized in Fig. 3. For this comparison, inactivation was evaluated for currents elicited with 200-ms pulses to a test potential of +70 mV. The relative component of noninactivating current measured at +70 mV for WT and each mutant channel is plotted in Fig. 3A when Kv1.5 was expressed alone ("α", left-) or when Kv1.5 was coexpressed with Kvβ1.3 ("$\alpha + \beta$", right). The Kvβ1.3-induced change in inactivation of mutant channels was also compared with WT channels as a ratio and is plotted in Fig. 3B. This analysis revealed that five mutations in the S6 domain (V505A, I508A, L510A, V512A, and V516A) were most effective in inhibiting Kvβ1.3-induced inactivation. In contrast, T479A and T480A greatly enhanced Kvβ1.3-induced inactivation.

We found previously that mutation to Ala of two residues located at the base of the pore helix (Thr479, Thr480) decreased block of Kv1.5 channels by S0100176. Even the conservative substitution of these residues to Ser strongly decreased the potency of block (Decher et al., 2004). For example, T480S increased IC_{50} by 88-fold compared with 362-fold for T480A. In contrast to the drug, mutation 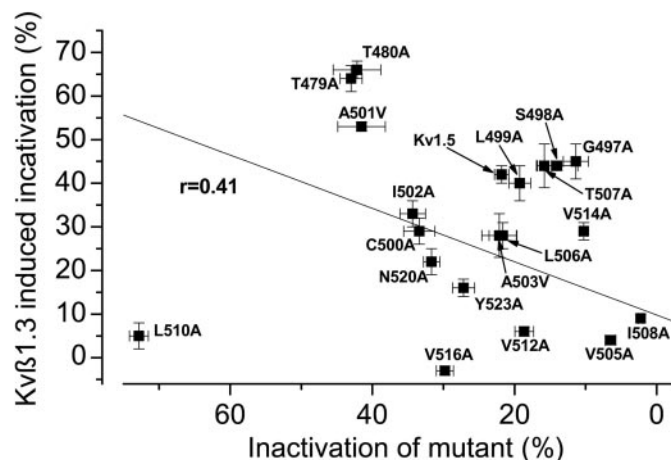of Thr479 or Thr480 to Ala enhanced the ability of Kvβ1.3 to induce inactivation, and this effect was accentuated when Thr480 was substituted with Ser (Fig. 4). Thus, mutation of Thr479 or Thr480 has opposite effects on the apparent binding affinities of S0100176 and Kvβ1.3 subunits.

N-type inactivation can enhance C-type inactivation (Baukrowitz and Yellen, 1995). Might there be a correlation between the rate of C-type inactivation induced by point mutations of the S6 domain of Kv1.5 and the extent of N-type inactivation induced by coexpression with Kvβ1.3? To test for such a correlation, the extent of inactivation during a 1.5-s pulse to +70 mV for Kv1.5 channels expressed alone or together with Kvβ1.3 subunits was compared and plotted in Fig. 5. This plot indicates that the extent of C-type inactivation of mutant Kv1.5 channels does not determine the ability of Kvβ1.3 to induce N-type inactivation.

Kvβ1.3 accelerated the rate of inactivation of WT and many mutant Kv1.5 channels during 1.5-s pulses. In the presence of Kvβ1.3 subunits, current inactivation for most channels was best fit with a biexponential function. The exceptions were V505A, I508A, V512A, and V516A (Fig. 6A). The inactivation of these four mutant channels were also examined using longer (5 s) pulses to +70 mV. With these longer pulses, inactivation was best fit with a biexponential function, but the rates were still slow and similar to those of WT Kv1.5 channels expressed alone (Fig. 6B). Thus, mutation of four residues in the S6 domain essentially eliminated the ability of Kvβ1.3 subunits to induce N-type inactivation of Kv1.5.

Deactivation of WT Kv1.5 was biexponential at −40 mV with time constants of 32.0 ± 1.1 and 9.2 ± 0.3 ms ($n = 15$). Coexpression with Kvβ1.3 slowed the deactivation of WT Kv1.5 by a factor of 2.35 ± 0.1 for the fast component and 1.95 ± 0.1 for the slow component (Fig. 6C, $n = 11$). Deactivation was also analyzed for −70 mV, and similar changes in deactivation rates were noted (Fig. 6D). The slowing of deactivation may result from an inability of the activation gate to close when a Kvβ ball peptide is bound to the inner pore of the channel. Consistent with this hypothesis, the effect of Kvβ1.3 on deactivation was minimal for channels harboring a mutation in V505A, I508A, L510A, or V512A residues in

Fig. 4. Mutation of Thr479 and Thr480 to Ala or Ser enhanced Kvβ1.3-induced in activation of Kv1.5 channels. A and B, example of currents for T480S Kv1.5 channels expressed alone or with Kvβ1.3 subunits. C, current measured at the end of 200-ms pulses to +70 mV was normalized relative to the peak initial current to obtain relative current for WT or mutant Kv1.5 channels coexpressed with Kvβ1.3 subunits. ##, $P < 0.001$ compared with WT Kv1.5+ Kvβ1.3.

Fig. 5. Lack of correlation between C-type inactivation of Kv1.5 and the ability of Kvβ1.3 to induce additional inactivation. Percentage inactivation during a 1.5-s pulse to +70 mV for Kv1.5 channels expressed alone (*x*-axis) is compared with that when Kv1.5 and Kvβ1.3 were coexpressed (*y*-axis).
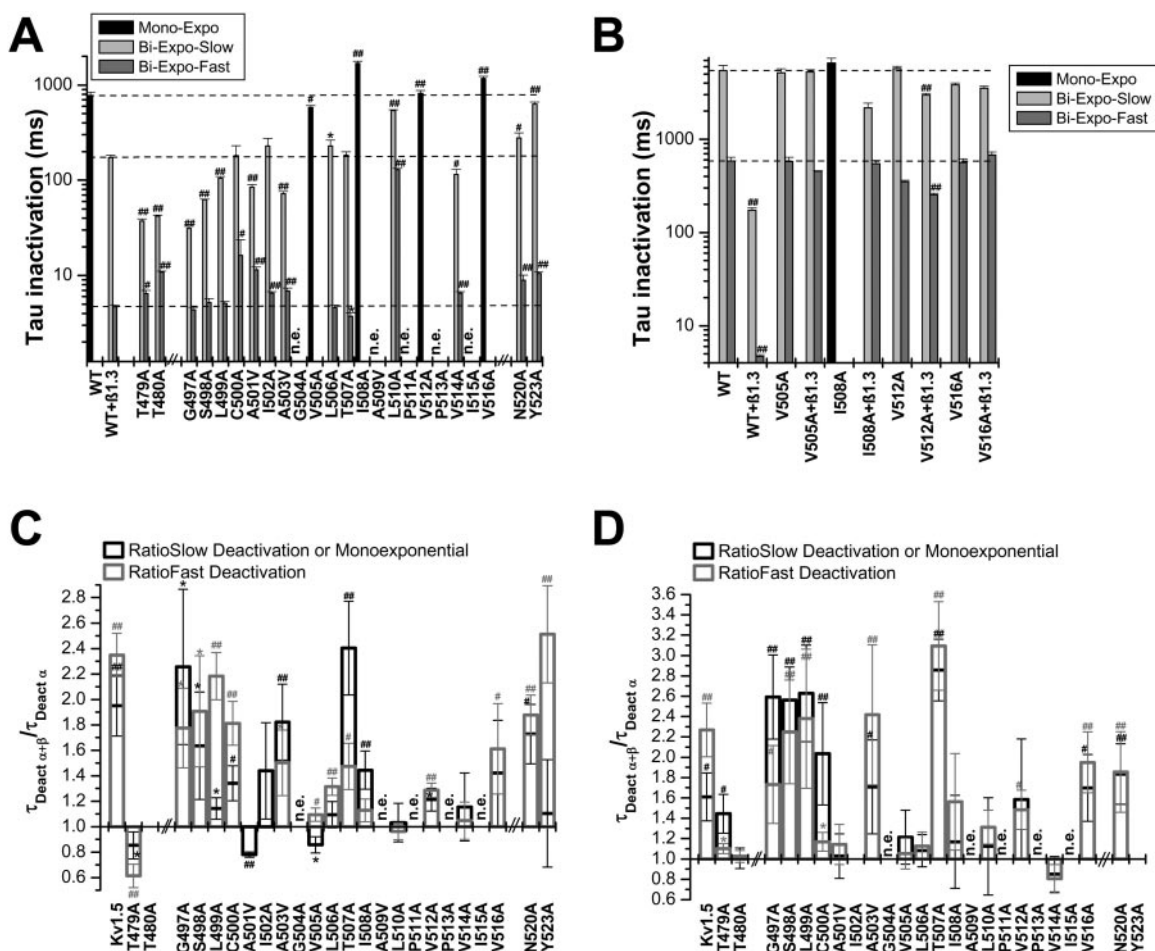
Fig. 6. Effects of Kv1.5 mutations on channel inactivation and deactivation. A, time constants for inactivation of WT and mutant Kv1.5 channels when coexpressed with Kvβ1.3. Currents during 1.5-s pulse to +70 mV were fit with either a mono- or biexponential function. *, $P < 0.05$; #, $P < 0.01$; ##, $P < 0.001$ compared with WT Kv1.5+ Kvβ1.3. B, time constants for inactivation of WT and select mutant Kv1.5 channels coexpressed with Kvβ1.3 during 5-s pulses to +70 mV. Currents were fit with either a mono- or biexponential function. *, $P < 0.05$; #, $P < 0.01$; ##, $P < 0.001$ for corresponding channels without Kvβ1.3. C and D, time constants for deactivation expressed as a ratio for currents measured at −40 mV (C) or −70 mV (D) in the presence or absence of Kvβ1.3 subunits. Deactivation of I502A was analyzed at −30 mV, and T480A channels were only analyzed at −70 mV. *, $P < 0.05$; #, $P < 0.01$; ##, $P < 0.001$ for corresponding channels without Kvβ1.3.
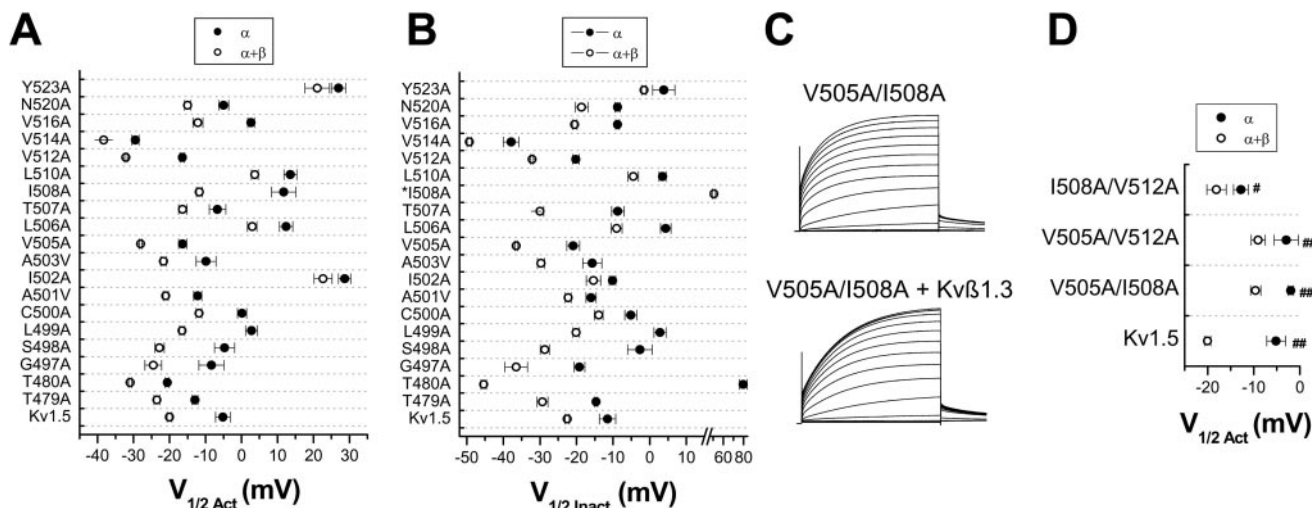
Fig. 7. Shifts in voltage dependence of Kv1.5 gating induced by coexpression with Kvβ1.3. Plot of half-point ($V_{1/2}$) for activation (A) and inactivation (B) of current determined for oocytes expressing Kv1.5 channels alone or when coexpressed with Kvβ1.3 subunits. C, Kvβ1.3 did not significantly alter properties of Kv1.5 channels formed from subunits containing two inactivation-perturbing mutations, V505A and I508A. D, Kvβ1.3-induced shift in $V_{1/2}$ for Kv1.5 activation is reduced but still present in channels that have two inactivation-perturbing mutations. #, $P < 0.01$; ##, $P < 0.001$ compared with corresponding channels without Kvβ1.3.

the S6 of Kv1.5 identified as crucial for interaction with Kvβ1.3. Deactivation of A501V, L506A, and V514A channels were also not affected much by coexpression with Kvβ1.3, but these mutations alone greatly slowed deactivation of Kv1.5 channels (Fig. 1).

Voltage-Dependent Shifts in Activation and Inactivation Gating Induced by Kvβ1.3 Are Independent of Interaction with the Inner Cavity of Kv1.5 Channels. Kvβ1.3 shifted the voltage required for half-maximal inactivation of Kv1.5 induced with 1.0-s test pulses by −11 mV. The $V_{1/2}$ was −11.5 ± 2.2 mV ($n = 12$) for Kv1.5 channels and −22.6 ± 0.6 mV ($n = 16$) for Kv1.5/Kvβ1.3 channels. In addition, Kvβ1.3 shifted the voltage dependence of activation by −15 mV, from −5.2 ± 2.0 mV ($n = 12$) to −20.0 ± 0.7 mV ($n = 18$). The Kvβ1.3-induced negative shifts in the half-points of the activation (Fig. 7A) and inactivation (Fig. 7B) relationships remained intact for most of the mutant Kv1.5 channels; in some cases (e.g., inactivation of T480A), they were exaggerated. The shifts in the voltage dependence of gating were also observed in most of the Kv1.5 channels harboring single mutations that abolished the Kvβ1.3-induced N-type inactivation (e.g., V505A, I508A, V512A, or V516A).
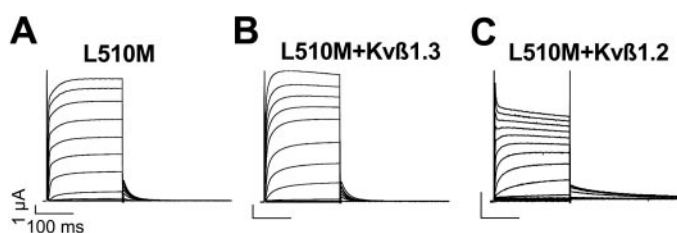
The combined mutation of two critical residues nearly eliminated the gating effects of Kvβ1.3. Coexpression with Kvβ1.3 had no apparent effect on gating of V505A/I508A (Fig. 7C), V505A/512A, or I508A/V512A channels, although a small shift in the voltage-dependence of C-type activation was still detected (Fig. 7D). Together, these findings suggest that although binding of Kvβ1.3 to the central cavity is likely to mediate N-type inactivation and a slowing of deactivation, binding to some other domain of Kv1.5 may mediate the negative shifts in the voltage dependence of activation and C-type inactivation.

Mutations of Leu510 in Kv1.5 Prevent Functional Interaction with Kvβ1.3 but Not Kvβ1.2 Subunits. With the exception of Leu510, the residues of the Kv1.5 subunit that seem to interact with Kvβ1.3 face toward the inner cavity of the channel. Of the mutations studied here, the L510A mutation caused the most pronounced enhancement of C-type inactivation, reducing current by 80% during a 1.5-s pulse to +70 mV. This mutation also prevented the slowing of deactivation normally associated with coexpression with Kvβ1.3. In contrast, mutation of Leu510 to Met slowed the rate of Kv1.5 activation but did not enhance C-type inactivation (Fig. 8A). Similar to L510A, Kvβ1.3 was unable to induce N-type inactivation of L510M channels (Fig. 8B). However, the L510M mutation did not prevent interaction of Kv1.5 with all Kvβ subunits because coexpression with Kvβ1.2 induced N-type inactivation and slowed the rate

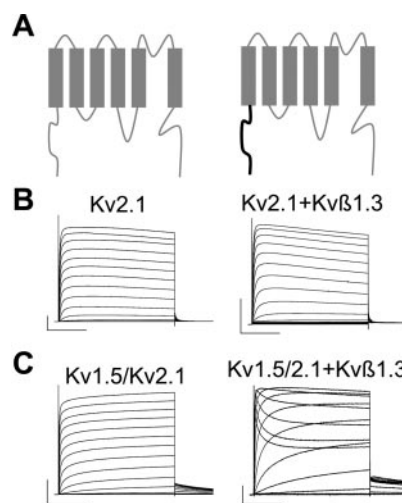of deactivation (Fig. 8C). Thus, mutation of Leu510 to Met prevented interaction with Kvβ1.3 but not Kvβ1.2 subunits, suggesting a Kvβ1-subunit–specific role for Leu in this position.

Sensitivity to Kvβ1 Requires both N-Terminal and Pore Domain Binding Sites. The sequence of the S6 domain is highly conserved in Kv1, -2, -3, and -4 α-subunits and the residues that face the central cavity, corresponding to Val505, Ile508, and Val512 of Kv1.5, are identical. However, Kvβ subunits are tethered to the channel complex by binding to a specific site located on the N terminus of some but not all Kv α-subunits. Kv2.1 α-subunits lack this N-terminal binding site for Kvβ subunits. Therefore, we constructed a Kv1.5-Kv2.1 chimera, combining the N terminus of Kv1.5 with the remaining domains of Kv2.1 (Fig. 9A). Kvβ1.3 had no effect on Kv2.1 gating (Fig. 9B) but induced N-type inactivation of the chimera channel (Fig. 9C), thus providing the Kv2.1 channel with an N terminus that could bind Kvβ1.3 enabled N-type inactivation.

Competition between Kvβ1.3 and a Drug for Binding to the Pore of Kv1.5 Channels. The time-dependent block of Kv1.5 channels by S0100176 roughly resembles Kvβ subunit-induced inactivation (Fig. 10A). As reported previously for bupivacaine and quinidine (Gonzalez et al., 2002), coexpression with Kvβ1.3 reduces the potency of S0100176 for block of Kv1.5 channels. At a test potential of +40 mV, the IC_{50} of S010076 for Kv1.5 currents was 0.7 ± 0.2 μM (Decher et al., 2004). In the presence of Kvβ1.3, the IC_{50} for block of channels was increased by more than 4-fold to 3.1 ± 0.2 μM ($n = 6$). Note that 1 μM drug blocked Kv1.5 channels more effectively than 3 μM drug blocked Kv1.5/Kvβ1.3 channels (Fig. 10A, top and middle). In addition, although block of Kv1.5 by S0100176 was voltage-independent over the range examined (−20 to +80 mV), block assumed a voltage-dependent profile in the presence of Kvβ1.3 (Fig. 10B, top and middle).


Fig. 9. N terminus and pore binding sites are required for Kvβ1.3-induced inactivation of Kv channels. A, schematic of Kv2.1 subunit (left) and Kv2.1 with Kv1.5 N terminus (right). B, Kvβ1.3 does not affect gating of Kv2.1. Currents were recorded during 1.5-s pulses applied from a holding potential of −80 mV to test potentials ranging from −60 to +90 mV. C, Kvβ1.3 induces inactivation of Kv2.1/Kv1.5 chimera channels. Currents were recorded using the same voltage protocols described for Kv2.1 currents. Scale bars in B and C represent 1 μA and 0.5 s.

Fig. 8. L510M mutation prevents interaction with Kvβ1.3 but not Kvβ1.2. L510M Kv1.5 currents were recorded at test potentials ranging from −60 to +70 mV (10-mV increments) in the absence (A) and presence of Kvβ1.3 (B) or Kvβ1.2 (C).

The N-terminal region of Kvβ subunits are believed to act as the inactivation ball (Uebele et al., 1998) and presumably can compete with drug for binding to specific residues in the pore of Kv1.5. Therefore, we determined whether deletion of the first 10 amino terminal amino acids of Kvβ1.3 altered its ability to compete with S0100176 for block of Kv1.5 channels. The IC_{50} of S0100176 for Kv1.5 in the presence of Kvβ1.3(ΔN1–10) was 0.9 ± 0.3 μM ($n = 5$), not significantly different from the IC_{50} for Kv1.5 alone. As predicted, Kvβ1.3(ΔN1–10) did not confer voltage-dependence to block of Kv1.5 by S0100176 (Fig. 10B, bottom). The $V_{1/2act}$ was −5.2 mV ± 2.0 for Kv1.5 ($n = 12$) compared with −14.0 ± 1.8 mV ($n = 5$) for Kv1.5/Kvβ1.3(ΔN1–10) ($P < 0.001$). Thus, although N-truncated Kvβ1.3 did not alter the IC_{50} or voltage dependence of Kv1.5 block by the drug, it retained the ability to shift the voltage dependence of Kv1.5 activation.

The onset of drug block was determined by plotting the $I_{drug}/I_{control}$ ratio as a function of time during a single pulse to +70 mV (Fig. 10C). The rate of current reduction by S0100176 was slower in the presence of Kvβ1.3 but not in the presence of Kvβ1.3(ΔN1–10), findings consistent with competition between drug and the WT Kvβ-subunit for a common binding site.

The time course for the recovery from Kvβ1.3-induced inactivation and/or block by the drug was assessed with a double-pulse protocol. Oocytes were depolarized to +40 mV for 1 s to induce inactivation and/or block, allowed to recover at −90 mV for a variable time, then pulsed again to +40 mV to assess the extent of channel recovery. Kv1.5/Kvβ1.3 channels inactivated 40% over 1 s during the first pulse to +40 mV, and current magnitude was almost fully recovered after only 30 ms at −90 mV (Fig. 11, ○). In the presence of drug, the recovery of Kv1.5 channel current from block (Fig. 11, ▲) was very slow, with a time constant of 486 ± 9 ms ($n = 5$) and only 4.6% recovery after 30 ms. In contrast, the time course for recovery from inactivation plus block of Kv1.5/Kvβ1.3 channels was biphasic (Fig. 11, ■). Current was recovered by 25.4% after 30 ms at −90 mV, and the fast component had a time course similar to the recovery from N-type inactivation induced by Kvβ1.3. Thus, N-type inactivation was reduced 40% in the presence of the drug. The slow component (unblock by drug) had a time constant of 425 ± 7.3 ms ($n = 5$), similar to recovery from block of Kv1.5 channels alone. These findings provide further functional evidence that Kvβ1.3 subunits compete with S0100176 for block of Kv1.5 channels. These findings, when combined with the Ala-scanning mutagenesis results, suggest that the binding sites for S0100176 and Kvβ1.3 are composed of overlapping, but not identical residues that line the central cavity of the Kv1.5 channel (Fig. 12).
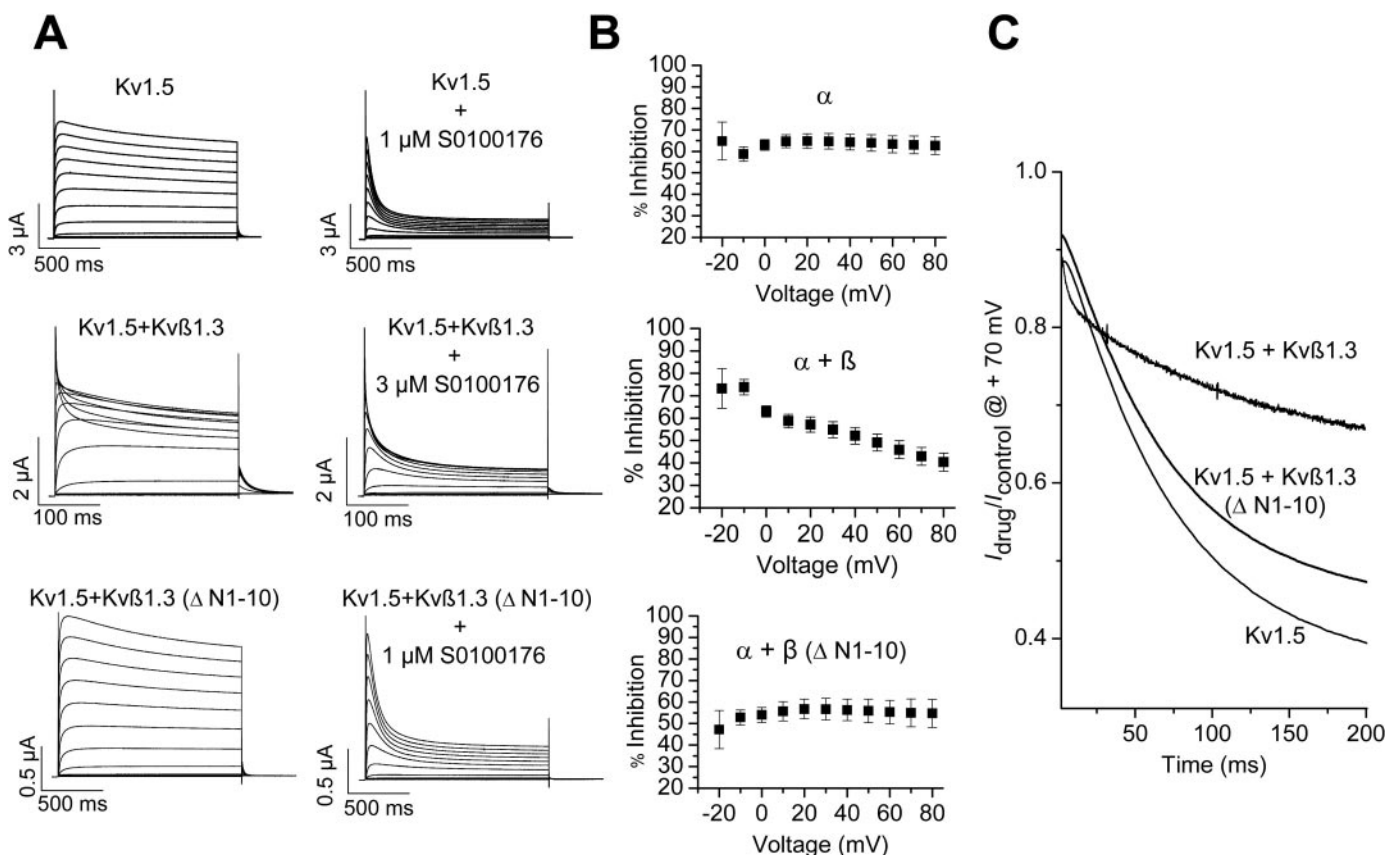
**Fig. 10.** Kvβ1.3 alters block of Kv1.5 channels by S0100176. A, WT Kv1.5, Kv1.5/Kvβ1.3, and Kv1.5/Kvβ1.3(ΔN1–10) channel currents recorded in the absence and presence of 1 μM S0100176. Currents were recorded during 1.5-s test pulses to potentials ranging from −20 to +80 mV. B, inhibition of currents by S0100176 as a function of voltage of the test pulse. Drug concentrations were chosen based on equivalent channel block at 0 mV. Plot for Kv1.5 alone + 1 μM S0100176 (top) was previously published (Decher et al., 2004). C, onset of current block at +70 mV for Kv1.5 and Kv1.5/Kvβ1.3(ΔN1–10) channels by 1 μM S0100176 and for Kv1.5/Kvβ1.3 by 3 μM S0100176. Currents recorded in the presence of drug were divided by currents recorded before exposure of the oocyte to drug to obtain the ratio $I_{drug}/I_{control}$.

Discussion

Kv1.5 channels activate rapidly and inactivate very slowly by a C-type mechanism. When coexpressed with Kvβ1 subunits, Kv1.5 channels acquire an additional and much more rapid N-type inactivation (England et al., 1995), a mode of inactivation dependent on a N-terminal inactivation peptide first identified at the molecular level in Shaker K$^+$ channels (Hoshi et al., 1990; Zagotta et al., 1990). More recently, Zhou et al. (2001) determined the molecular mechanism of N-type inactivation for a Kvβ1.1-β2 chimera subunit and an inactivation removed Kv1.4 channel, Kv1.4-IR. These investigators used a mutagenesis approach to identify important residues for N-type inactivation in both the α- and β-subunits. Zhou et al. (2001) mutated the six residues of Kv1.4-IR that were predicted to face the inner cavity based on a sequence alignment with KcsA. These individual mutations affected both the K_d of Kvβ1-induced inactivation and the K_d for
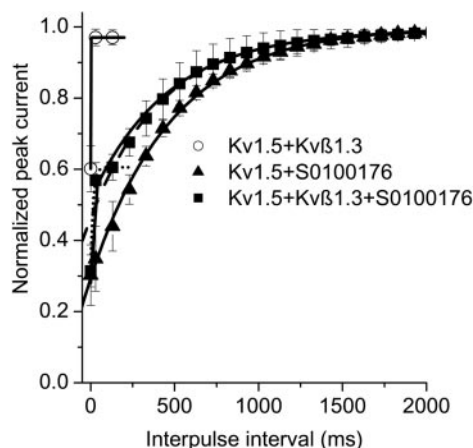

Fig. 11. Time-dependent recovery from block by S0100176 for Kv1.5 and Kv1.5/Kvβ1.3 channels. Normalized peak current amplitudes are plotted versus the interpulse time at −90 mV for Kv1.5 + Kvβ1.3 (○), Kv1.5 + S0100176 (▲), and Kv1.5 + Kvβ1.3 +3 μM S0100176 (■). Oocytes were depolarized by stepping for 1 s to +40 mV before return to the holding potential of −90 mV. After a range of times at −90 mV, a second depolarizing pulse was applied to +40 mV. The time course for recovery from inactivation of Kv1.5/Kvβ1.3 channels and recovery from block of Kv1.5 by S0100176 were fit with a mono-exponential function. The recovery from block/inactivation of Kv1.5/Kvβ1.3 channels in the presence of 3 μM S0100176 was fit with a biexponential function, reflecting fast recovery from inactivation (dotted curve) and slow recovery from block (dashed curve).

block of the channel by tetrabutylammonium (TBA). They noted that the volume of the first three residues of the Kvβ1.1 peptide (MQV) was similar to the volume of TBA, implying that the peptide and the TBA bind to the same receptor site in the Kv1.4-IR pore. Zhou et al. (2001) also proposed that interaction of the Kvβ1.1 N-terminal peptide with the Kv1.4-IR pore required two sequential gating steps between two open (O, O′) and one inactivated (I) state of the channel: O → O′ → I. The N terminus of a single Kvβ1 subunit initially binds to a site outside the pore, perhaps by snaking its way through a window in the T1-S1 linker. The transition from the open channel (O) to the preinactivated state (O′) was shown to be the rate-limiting step in the inactivation pathway. The more rapid and final transition (O′ → I) was proposed to result from binding of the Kvβ1.1 N terminus (residues MQVSIA) to specific residues of S6 that face the central cavity.

The S6 sequence of Kv1.4-IR and Kv1.5 channels is identical, whereas the initial N-terminal sequence of Kvβ1.3 is MLAART. Thus, it was unknown whether binding of Kvβ1.3 to the S6 domain of Kv1.5 would be the same as in the Zhou et al. study. In fact, there are several differences between our findings and the previous study. Our coexpression of mutant Kv1.5 channels with Kvβ1.3 identified five residues in the S6 segment and two residues located at the base of the pore helix as important interaction sites for Kvβ1.3, whereas Zhou et al. (2001) only investigated residues in S6 that were predicted to face the central cavity and therefore did not mutate Leu556 in Kv1.4-IR or the two Thr residues at the base of the pore helix. Thus, our data suggest that Kvβ1.3 may bind higher in the pore than predicted by the earlier study. Moreover, whereas Zhou et al. (2001) identified Tyr569 as one of the most important residues for Kvβ binding to Kv1.4, mutation of Tyr523 in Kv1.5 only modestly affected Kvβ1.3 interaction. The residues in S6 crucial for interaction with Kvβ subunits are underlined, and the differences in the putative binding-site deduced in the two studies are bold and italic:

Kv1.4+β1.1-β2.1: 551 <u>V</u>LT<u>I</u><u>A</u>LP<u>V</u>PVI<u>V</u>SNFNYF***Y*** 569
Kv1.5+β1.3:   505 <u>V</u>LT<u>I</u><u>A</u>*L*P<u>V</u>PVI<u>V</u>SNFNYFY 523

Leu510 of Kv1.5 is predicted to face away from the central cavity. We previously found that L510A had no effect on block of Kv1.5 by the anthranilic acid derivative S0100176 (Decher et al., 2004). Therefore, we were somewhat surprised to discover that mutation of this residue greatly diminished
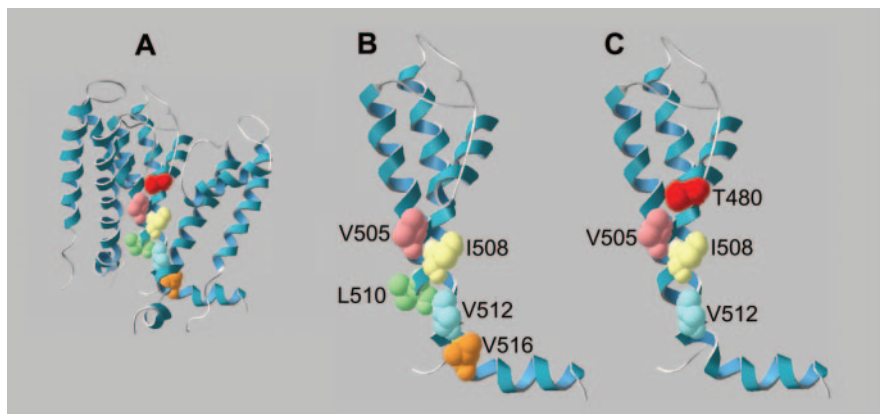
Fig. 12. Partial overlap of drug and Kvβ1.3 binding sites on S6 domain of Kv1.5 channel subunit. A, model of the Kv1.5 channel pore depicting three subunits. Model is tilted from the horizontal axis to facilitate viewing of residues important for interaction with Kvβ1.3 and S0100176 plotted on one of the subunits. The S5-S6 domains of a single Kv1.5 subunit are depicted with important residues for interaction with Kvβ1.3 (B) or S0100176 (C) highlighted in space-fill mode. Interacting residues are defined by a mutation-induced decrease in the extent of inactivation caused by Kvβ1.3 or a decrease in block by drug. In addition, mutation of Thr479 or Thr480 enhanced the ability of Kvβ1.3 to inactivate Kv1.5 channels. Homology models are based on the crystal structure of the KcsA channel (Doyle et al., 1998), incorporating a predicted bending of the S6 domain at the PVP motif (Hanner et al., 2001; Decher et al., 2004).

the ability of Kvβ1.3 subunits to alter Kv1.5 channel gating. However, mutation of Leu510 was previously reported to decrease channel block by the local anesthetics quinidine and tetraethylammonium (Yeola et al., 1996; Franqueza et al., 1997; Caballero et al., 2002).

Mutation of Val516 to Ala caused the greatest impairment of Kvβ1.3-induced inactivation of Kv1.5 channels. A similar mutation in Kv1.1 channels causes episodic ataxia type-1 (Browne et al., 1994), and heterozygous (V408A/+) transgenic mice developed stress-induced loss of motor coordination (Herson et al., 2003). Similar to V516A in Kv1.5, the V408A mutation in Kv1.1 caused a 10-fold increase in the rate of Kv1.1 deactivation and greatly slowed the rate of Kvβ-induced inactivation (Adelman et al., 1995; Maylie et al., 2002). Thus, mutation of this critical Val in the S6 domain of Kv1 channels prevents normal interaction with Kvβ subunits.

In addition to inducing N-type inactivation, Kvβ1.3-induces a negative shift in the voltage dependence of Kv1.5 channel activation and inactivation. We found that most mutations in the S6 of Kv1.5 that prevented Kvβ1.3-mediated N-type inactivation did not prevent shifts in the voltage dependence of gating. The structural basis of the shifts in gating are unknown, but the shifts remain largely intact when the 68 amino acids are removed from the N terminus of the β-subunit, implying that different domains of Kvβ1.3 are responsible for inducing rapid inactivation and shifting the voltage dependence of gating of Kv1.5 channels (Uebele et al., 1998). Our results also suggest that a domain of Kv1.5 that is located outside the pore may be involved in the gating effects. Perhaps the shifts in gating correspond to the transition from the open to the preinactivated state (O $\rightarrow$ O′) proposed in the Zhou et al. (2001) model of Kv1 channel gating.

Specific mutations of Kv1.5 (Val514, Thr507) that increased block by quinidine did not alter Kvβ1.3-induced inactivation, suggesting that the drug binding site is distinct from the one that mediates fast inactivation (Uebele et al., 1998). However, our Ala-scanning studies suggest a similar binding site for an anthranilic acid derivative S0100176 and the peptide inactivation gate of Kvβ1.3. Thr480 (and to a lesser extent Thr479), located at the base of the pore helix, and Val505, Ile508, and Val512, located in S6, were identified as the putative binding sites for this drug. Based on altered properties of inactivation induced by mutation, these same residues mediate interaction with Kvβ1.3 subunits. In addition, Kvβ1.3 seems to interact with Leu510 and Val516 on the S6 domain. Finally, Kvβ1.3 (but not an N-truncated construct) reduced the potency of S0100176 block and converted the profile from voltage-independent to voltage-dependent. Together, these findings strongly suggest that the blocker and the Kvβ1.3 subunit compete for an overlapping but not identical binding site located in the inner cavity of Kv1.5.

References

Adelman JP, Bond CT, Pessia M, and Maylie J (1995) Episodic ataxia results from voltage-dependent potassium channels with altered functions. *Neuron* **15:**1449–1454.

Antz C and Fakler B (1998) Fast inactivation of voltage-gated K⁺ channels: from cartoon to structure. *News Physiol Sci* **13:**177–182.

Antz C, Geyer M, Fakler B, Schott MK, Guy HR, Frank R, Ruppersberg JP, and Kalbitzer HR (1997) NMR structure of inactivation gates from mammalian voltage-dependent potassium channels. *Nature (Lond)* **385:**272–275.

Armstrong CM (1981) Sodium channels and gating currents. *Physiol Rev* **61:**644–683.

Baukrowitz T and Yellen G (1995) Modulation of K⁺ current by frequency and external [K⁺]: a tale of two inactivation mechanisms. *Neuron* **15:**951–960.

Browne DL, Gancher ST, Nutt JG, Brunt ERP, Smith EA, Kramer P, and Litt M (1994) Episodic ataxia/myokymia syndrome is associated with point mutations in the human potassium channel gene, KCNA1. *Nat Genet* **8:**136–140.

Caballero R, Moreno I, Gonzalez T, Valenzuela C, Tamargo J, and Delpon E (2002) Putative binding sites for benzocaine on a human cardiac cloned channel (Kv1.5). *Cardiovasc Res* **56:**104–117.

Coetzee WA, Amarillo Y, Chiu J, Chow A, Lau D, McCormack T, Moreno H, Nadal MS, Ozaita A, Pountney D, et al. (1999) Molecular diversity of K⁺ channels. *Ann NY Acad Sci* **868:**233–285.

De Biasi M, Wang Z, Accili E, Wible B, and Fedida D (1997) Open channel block of human heart hKv1.5 by the beta-subunit hKvβ1.2. *Am J Physiol* **272:**H2932–H2941.

Decher N, Pirard B, Bundis F, Peukert S, Baringhaus KH, Busch AE, Steinmeyer K, and Sanguinetti MC (2004) Molecular basis for Kv1.5 channel block: conservation of drug binding sites among voltage-gated K⁺ channels. *J Biol Chem* **279:**394–400.

Doyle DA, Morais Cabral J, Pfuetzner RA, Kuo A, Gulbis JM, Cohen SL, Chait BT, and MacKinnon R (1998) The structure of the potassium channel: molecular basis of K⁺ conduction and selectivity. *Science (Wash DC)* **280:**69–77.

England SK, Uebele VN, Kodali J, Bennett PB, and Tamkun MM (1995) A novel K⁺ channel β-subunit (hKvβ1.3) is produced via alternative mRNA splicing. *J Biol Chem* **270:**28531–28534.

Fink M, Duprat F, Lesage F, Heurteaux C, Romey G, Barhanin J, and Lazdunski M (1996) A new K⁺ channel beta subunit to specifically enhance Kv2.2 (CDRK) expression. *J Biol Chem* **271:**26341–26348.

Franqueza L, Longobardo M, Vicente J, Delpon E, Tamkun MM, Tamargo J, Snyders DJ, and Valenzuela C (1997) Molecular determinants of stereoselective bupivacaine block of hKv1.5 channels. *Circ Res* **81:**1053–1064.

Giese KP, Storm JF, Reuter D, Fedorov NB, Shao LR, Leicher T, Pongs O, and Silva AJ (1998) Reduced K⁺ channel inactivation, spike broadening and afterhyperpolarization in Kvβ1.1-deficient mice with impaired learning. *Learn Mem* **5:**257–273.

Gonzalez T, Navarro-Polanco R, Arias C, Caballero R, Moreno I, Delpon E, Tamargo J, Tamkun MM, and Valenzuela C (2002) Assembly with the Kvβ1.3 subunit modulates drug block of hKv1.5 channels. *Mol Pharmacol* **62:**1456–1463.

Hanner M, Green B, Gao YD, Schmalhofer WA, Matyskiela M, Durand DJ, Felix JP, Linde AR, Bordallo C, Kaczorowski GJ, et al. (2001) Binding of correolide to the Kv1.3 potassium channel: characterization of the binding domain by site-directed mutagenesis. *Biochemistry* **40:**11687–11697.

Herson PS, Virk M, Rustay NR, Bond CT, Crabbe JC, Adelman JP, and Maylie J (2003) A mouse model of episodic ataxia type-1. *Nat Neurosci* **6:**378–383.

Hoshi T, Zagotta WN, and Aldrich RW (1990) Biophysical and molecular mechanisms of *Shaker* potassium channel inactivation. *Science (Wash DC)* **250:**533–538.

Leicher T, Bahring R, Isbrandt D, and Pongs O (1998) Coexpression of the KCNA3B gene product with Kv1.5 leads to a novel A-type potassium channel. *J Biol Chem* **273:**35095–35101.

Maylie B, Bissonnette E, Virk M, Adelman JP, and Maylie JG (2002) Episodic ataxia type 1 mutations in the human Kv1.1 potassium channel alter hKvβ1-induced N-type inactivation. *J Neurosci* **22:**4786–4793.

Peukert S, Brendel J, Pirard B, Bruggemann A, Below P, Kleemann HW, Hemmerle H, and Schmidt W (2003) Identification, synthesis and activity of novel blockers of the voltage-gated potassium channel Kv1.5. *J Med Chem* **46:**486–498.

Rhodes KJ, Strassle BW, Monaghan MM, Bekele-Arcuri Z, Matos MF, and Trimmer JS (1997) Association and colocalization of the Kvβ1 and Kvβ2 β-subunits with Kv1 α-subunits in mammalian brain K⁺ channel complexes. *J Neurosci* **17:**8246–8258.

Sarkar G and Sommer SS (1990) The "megaprimer" method of site-directed mutagenesis. *BioTechniques* **8:**404–407.

Sewing S, Roeper J, and Pongs O (1996) Kvβ1 subunit binding specific for shaker-related potassium channel alpha subunits. *Neuron* **16:**455–463.

Snyders DJ and Yeola SW (1995) Determinants of antiarrhythmic drug action. Electrostatic and hydrophobic components of block of the human cardiac hKv1.5 channel. *Circ Res* **77:**575–583.

Stuhmer W (1992) Electrophysiological recording from *Xenopus* oocytes. *Methods Enzymol* **207:**319–339.

Uebele VN, England SK, Gallagher DJ, Snyders DJ, Bennett PB, and Tamkun MM (1998) Distinct domains of the voltage-gated K⁺ channel Kvβ1.3 β-subunit affect voltage-dependent gating. *Am J Physiol* **274:**C1485–C1495.

Vennekamp J, Wulff H, Beeton C, Calabresi PA, Grissmer S, Hansel W, and Chandy KG (2004) Kv1.3-blocking 5-phenylalkoxypsoralens: a new class of immunomodulators. *Mol Pharmacol* **65:**1364–1374.

Yang EK, Alvira MR, Levitan ES, and Takimoto K (2001) Kvβ subunits increase expression of Kv4.3 channels by interacting with their C termini. *J Biol Chem* **276:**4839–4844.

Yeola SW, Rich TC, Uebele VN, Tamkun MM, and Snyders DJ (1996) Molecular analysis of a binding site for quinidine in a human cardiac delayed rectifier K$^+$ channel. *Circ Res* **78:**1105–1114.

Zagotta WN, Hoshi T, and Aldrich RW (1990) Restoration of inactivation in mutants of Shaker potassium channels by a peptide derived from ShB. *Science (Wash DC)* **250:**568–571.

Zhou M, Morais-Cabral JH, Mann S, and MacKinnon R (2001) Potassium channel receptor site for the inactivation gate and quaternary amine inhibitors. *Nature (Lond)* **411:**657–661.

Address correspondence to: Michael C. Sanguinetti, Nora Eccles Harrison Cardiovascular Research and Training Institute, University of Utah, 95 S 2000 E, Salt Lake City, UT 84112. E-mail: sanguinetti@cvrti.utah.edu